

CrossMark
click for updatesCite this: *J. Mater. Chem. A*, 2016, 4, 1608Received 5th November 2015
Accepted 23rd December 2015

DOI: 10.1039/c5ta08945j

www.rsc.org/MaterialsA

Carbodiimides: new materials applied as anode electrodes for sodium and lithium ion batteries†

A. Eguía-Barrio,^a E. Castillo-Martínez,^{*b} X. Liu,^c R. Dronskowski,^c M. Armand^b and T. Rojo^{*ab}

Conversely to the electrochemical inactivity claimed for MnNCN, we report here that transition-metal carbodiimides, MNCN (M = Cu, Zn, Mn, Fe, Co and Ni), are electrochemically active materials for electrochemical energy-storage systems. They exhibit high reversible capacities (200–800 mA h g^{−1}) for lithium and sodium ion batteries, stored by means of conversion reactions.

At the beginning of the 21st century, exploiting the so-called “renewable” energies has become another focus of energy-related research. A severe issue associated with “renewables” is that generation and consumption does not occur at the same time. In principle, however, energy can be stored in portable or stationary devices such as batteries at production peaks in order to fully take advantage of the stored “renewable” energy when needed.¹

Due to the high energy density of lithium ion batteries (LIBs), these devices are at the center of the portable electronics markets. On the other hand, work on sodium ion batteries (SIBs) is being carried out mostly for stationary applications. The search for new electrode materials is important in order to improve the safety and environmental aspects of batteries, lower the costs or improve cycle life or energy density of batteries. Until now, graphite is the preferred anode material for lithium ion batteries taking into account its good chemical, thermal and mechanical stability,² amount of stored energy and price for lithium ion batteries. Nonetheless, for sodium ion batteries,^{3,4} “naked” sodium ions are unable to intercalate in graphite unless the electrolyte solvent, if of sufficient donor

number (DN), is co-intercalated.⁵ Although there is still no material which can provide as good electrochemical properties for SIBs as graphite does for LIBs, hard carbons present good performance and seem to be the best anode materials for sodium ion batteries.⁶ Moreover, in order to lower the price of the synthetic process, research in organic compounds such as terephthalates⁷ or polymers as Schiff bases⁸ has started. Some inorganics such as red phosphorus⁹ or tin¹⁰ and antimony¹¹ alloys show large plateaus with a high reversible capacity at low voltages but they lead to unsafe products XH₃ (X = P, Sb) and tin resources are largely depleted. We have decided to investigate transition-metal carbodiimides due to their similarities to the corresponding oxides. Both anions have the same charge (2−) and similar electronegativity values, namely 3.36 for NCN and 3.47 for O.¹² The lower electronegativity value of the (N=C=N) group and larger charge delocalization cause its bond with the transition metals to be more covalent¹³ in comparison with the oxide bonds. Also, the structures of transition-metal carbodiimides and oxides are often similar with a small distortion due to the larger size of the NCN group (Fig. 1). Most of the metal carbodiimides have a [N=C=N]^{2−} group configuration following the Pearson HSAB principle.¹⁴ The transition-metal

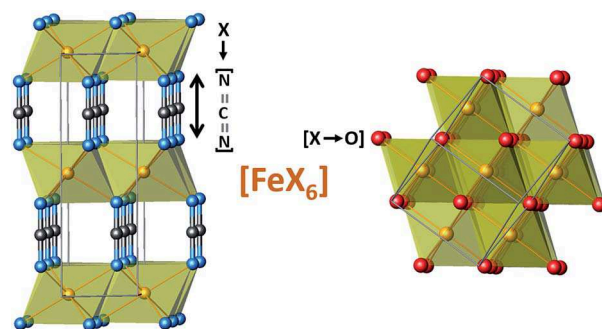


Fig. 1 FeNCN (left) and FeO (right) structures. Octahedra of FeX₆ are drawn in both structures. The splitting of the layers of FeX₆ octahedra is pointed in the carbodiimide (left).

^aDepartment of Inorganic Chemistry, University of Basque Country, Barrio Sarriena s/n, P.O. Box 644, 48080 Bilbao, Spain. E-mail: teo.rojo@ehu.es

^bCIC EnergiGUNE, Parque Tecnológico de Álava, C/Albert Einstein 48, 01510, Miñano, Spain. E-mail: ilaisza@hotmail.com

^cInstitute of Inorganic Chemistry, RWTH Aachen University, Landoltweg 1, D-52056 Aachen, Germany

† Electronic supplementary information (ESI) available: Additional experimental details, spectroscopic study and structural characterization including Fig. S1–S3 and Tables S1 and S2. See DOI: 10.1039/c5ta08945j

ions M^{2+} studied in this paper prefer the carbodiimide $[N=C=N]^{2-}$ form than the cyanamide $[N-C\equiv N]^{2-}$ configuration.¹⁵ However, H_2NCN has the $[N-C\equiv N]^{2-}$ configuration because the molecule is stabilized through the presence of hydrogen bonds. Moreover, the low molecular weight of the bivalent transition-metal carbodiimides makes them good candidates as anode materials. They have relatively high theoretical capacities (between 254 mA h g^{-1} per Li or Na ion in $ZnNCN$ and 282 mA h g^{-1} in $MnNCN$). Analogue oxides such as CuO ,¹⁶ MnO ,¹⁷ FeO ,¹⁸ CoO ¹⁹ or NiO ¹⁶ react through conversion reaction mechanisms for lithium ion batteries. Nonetheless, for sodium ion batteries, FeO , CoO and NiO seem to be almost electrochemically inactive.²⁰ Given the similarities between both families and the “softer” chemical character of CN vs. O (bases), an improvement in the electrochemical behaviour may be expected. Until now, transition-metal carbodiimides $MNCN$ ($M = Cu, Zn, Mn, Fe, Co$, and Ni) were only explored in terms of their magnetic properties. We here report the first electrochemically active carbodiimide materials for both lithium and sodium ion batteries.

Copper²¹ and zinc¹⁵ carbodiimides were prepared in aqueous media from metal chlorides and cyanamide. Manganese carbodiimide was prepared by a new metathesis reaction of lithium carbodiimide and manganese chloride in stoichiometric amounts using THF as the solvent. Lithium carbodiimide was synthesized with butyl-lithium and cyanamide as precursors with a ratio of 2.4 : 1. However, iron,²² cobalt and nickel carbodiimides²³ were obtained in two-step reactions. The first step was based on the synthesis of the metal hydrogen dicyanamide in aqueous media using the metal chlorides and cyanamide. The second step is the synthesis of the metal carbodiimide in a sealed glass ampoule. The metal hydrogen dicyanamide is mixed with a mixture of lithium and potassium chloride at the eutectic composition (59 : 41, mp = 352°C) and heated up to 400°C , melamine from disproportionation condensing at the cold end. The synthesized carbodiimides were structurally and electrochemically characterized. $MNCN$ with $M = Cu, Zn, Mn, Fe, Co$, and Ni were obtained as a pure phase as confirmed by XRD (Fig. 2).

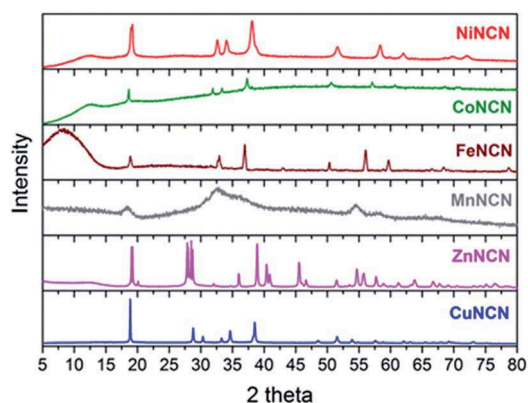


Fig. 2 X-Ray diffraction patterns of nickel (red), cobalt (green), iron (brown), manganese (grey), zinc (pink) and copper (blue) carbodiimide.

$CuNCN$ and $ZnNCN$ reflect a better crystallinity than $FeNCN$, $CoNCN$ and $NiNCN$. $MnNCN$, synthesized by a new metathesis route from Li_2NCN and $MnCl_2$, has a very small particle size (6 nm) as deduced from the Debye–Scherrer equation. The refined cell parameters of the synthesized carbodiimides are listed in Table S1.† Also, the most typical IR bands of carbodiimides (the asymmetrical stretching vibration at $2000\text{--}2100\text{ cm}^{-1}$ and the strong deformation at $600\text{--}700\text{ cm}^{-1}$) are all in agreement with the reported values.²⁴ The infrared spectra can be seen in Fig. S1† and the frequencies at which these bands appear are listed in Table S2.† The large shift in the asymmetrical stretching of H_2NCN ²⁴ is due to the cyanamide $[N-C\equiv N]^{2-}$ configuration with the asymmetrical stretching of H_2NCN appearing at 2200 cm^{-1} and being absent in all $MNCN$.

The electrochemical performance of carbodiimides for SIB and LIB applications is represented in Fig. 3. All tested carbodiimides display high reversible capacity values ($200\text{--}800\text{ mA h g}^{-1}$) for both sodium and lithium ions at voltages down to $0.005\text{ V vs. Li}^+/\text{Li}$ or $\text{vs. Na}^+/\text{Na}$. $FeNCN$, $CoNCN$ and $NiNCN$ showed capacities close to the theoretical ones for the insertion of 2 ions.

Nevertheless, it has to be taken into account that the reduction goes down to $0.005\text{ V vs. Na}^+/\text{Na}$, so there is a contribution of the SEI layer formation to the irreversible capacity and also of the insertion into carbon to the reversible capacity since 20% of the electrode is carbon (Fig. S2†). A small amount of Ketjen black is needed for the materials which react at low voltages to be active. The smaller particle size and higher surface area of this carbon with respect to typical activated carbons provide better percolation enabling materials such as $ZnNCN$ and $MnNCN$ to be electrochemically active.

Herein, each carbodiimide shows its distinct behaviour. $NiNCN$ (red charts in Fig. 3) and $CoNCN$ (plotted in green) galvanostatic cycles have very similar properties for LIBs and SIBs and show the largest reversible and irreversible capacities in the first cycle. While in $NiNCN$ there is a very large plateau at $\sim 0.7\text{ V vs. Na}^+/\text{Na}$ and at $\sim 0.9\text{ V vs. Li}^+/\text{Li}$, $CoNCN$ has the plateau at $0.9\text{ V vs. Na}^+/\text{Na}$ and $1.1\text{ V vs. Li}^+/\text{Li}$. $CoNCN$ has a reversible capacity of about 600 mA h g^{-1} for sodium ion batteries, that is very close to the theoretical one for two electrons (542 mA h g^{-1}). For lithium-ion batteries, however, the capacity value is about 800 mA h g^{-1} , probably due to the larger contribution of the carbon for Li^+ insertion even if the amount of carbon in each electrode is more or less the same. However, $NiNCN$ has a capacity around $600\text{--}700\text{ mA h g}^{-1}$ for sodium and lithium ions which is a value close to the theoretical capacity for two electrons (543 mA h g^{-1}).

$FeNCN$, $MnNCN$, $ZnNCN$ and $CuNCN$ have smaller reversible capacity as well as smaller irreversible capacity in the first cycle. $FeNCN$ also exhibits less polarization and irreversible capacity both for Li and Na ions (brown lines in Fig. 3). It shows a reversible capacity of 450 mA h g^{-1} cycling vs. sodium with a very large plateau at $0.25\text{ V vs. Na}^+/\text{Na}$, and 550 mA h g^{-1} vs. lithium which corresponds to the theoretical capacity for transferring 2 electrons for $FeNCN$.

$MnNCN$ exhibits a very different behavior for SIBs and LIBs. For SIBs, it shows a reversible capacity of 200 mA h g^{-1} (grey

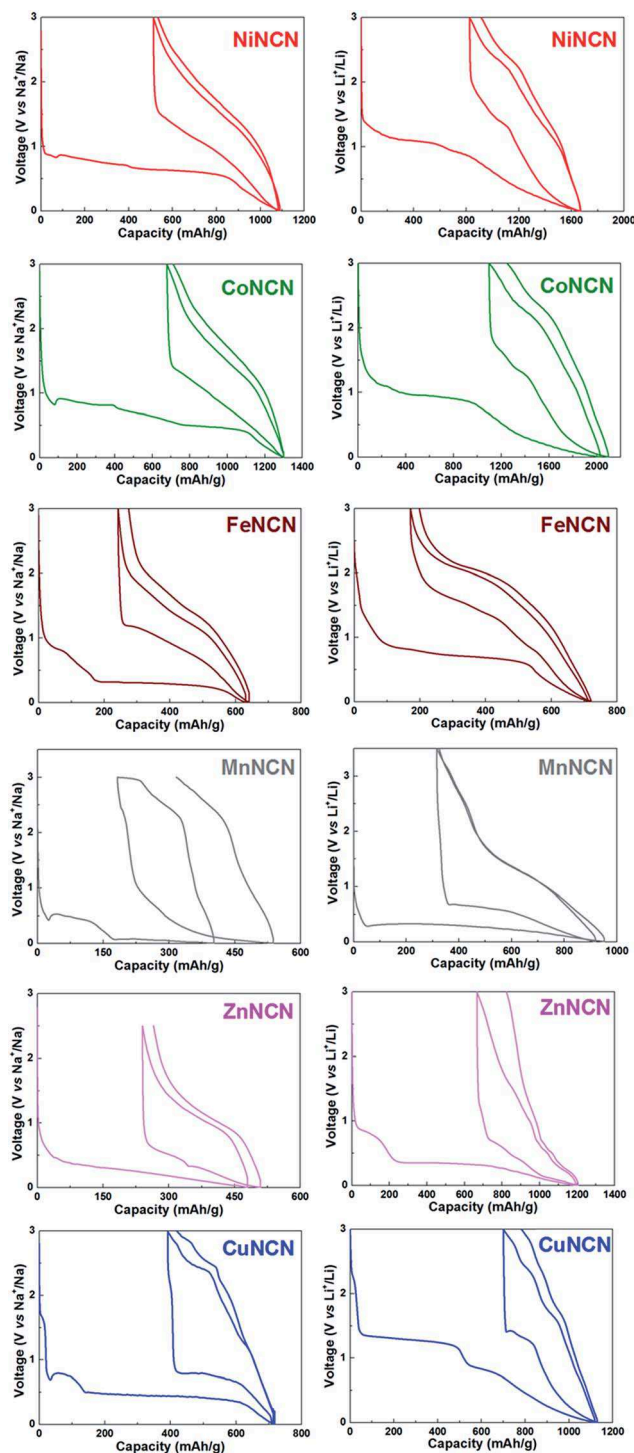


Fig. 3 Two first galvanostatic cycles with a constant current rate of $C/10$ of NiNCN (red), CoNCN (green), FeNCN (brown), MnNCN (grey), ZnNCN (pink) and CuNCN (blue) for sodium (left side) and lithium (right side) ion batteries. The materials were cycled with a constant current rate of $C/10$ considering $C = 2 \text{ Na}^+$ or Li^+ ions per MNCN unit.

chart of Fig. 3 on the left) although with very high polarization. Note that a proportion of high surface area carbon, Ketjen black, was needed in order to achieve activity vs. sodium. On the other hand, in a LIB, (Fig. 3 plotted in grey on the right) it

provides a very high reversible capacity of 600 mA h g^{-1} , very close to the theoretical one for 2 transferred electrons in MnNCN with a plateau at a very low voltage of $0.2 \text{ V vs. Li}^+/\text{Li}$ in the first discharge and at $0.5 \text{ V vs. Li}^+/\text{Li}$ for the next cycles, with smaller polarization. Also, it is worth mentioning that the MnNCN with a larger crystal size synthesized following the original method²⁵ is not electrochemically active.²⁶ ZnNCN, cycling vs. sodium and vs. lithium (pink lines in Fig. 3), has a reversible capacity of 250 mA h g^{-1} and one plateau at $0.5 \text{ V vs. A}^+/\text{A}$, irrespective of $A = \text{Li}^+$ or Na^+ , which is unexpected. Finally, CuNCN has a reversible capacity of 300 mA h g^{-1} with a big polarization for sodium ion batteries, indicated as a blue line in Fig. 3 on the left, similar to that reported for CuO vs. Na^+/Na ,²⁷ and smaller polarization and capacity (250 mA h g^{-1}) vs. Li^+/Li in blue line on the right in Fig. 3.

In order to better detect the voltages at which the redox reactions of all carbodiimide electrodes occur, $\delta Q/\delta V$ s of all of the MNCN are represented in Fig. S3a† for the first cycle. Along with the increase in the number of 3d electrons the average voltage of the reduction reaction of the carbodiimides is also increasing from MnNCN to FeNCN, CoNCN and NiNCN. However, CuNCN and ZnNCN do not follow the same rule because 4s orbitals are involved in the redox reactions.²⁸

Ex situ XRD patterns have been collected for all samples at the end of discharge (Fig. S4†). We present here, as a representative, the *in situ* XRD experiment of CuNCN during reduction (Fig. 4). When CuNCN is cycled vs. Na^+/Na , at the initial steps of Na^+ insertion, all the reflections corresponding to CuNCN decrease in intensity during cycling but they are not shifted. This proves that there is no topochemical Na^+ intercalation through a solid-solution process despite the sloppy character of the voltage curve. Later, during the $\sim 0.4 \text{ V vs. Na}^+/\text{Na}$ voltage plateau, the intensity of the reflections continues to decrease, although not monotonically, meaning that some side processes such as electrolyte decomposition and SEI layer formation occur simultaneously with the electrochemical reaction, although at different rates, in this voltage range. At the end of the discharge the reflections of CuNCN disappear while only a very broad peak appears at $2\theta \sim 44^\circ$. The latter corresponds to the (111) reflection of metallic copper which suggest that a conversion reaction similar to those occurring in oxides is taking place. The carbodiimide reflections were not recovered after the first charge (Fig. S5†). This suggests that the electrode material reacts towards a smaller particle size and from there, it is impossible

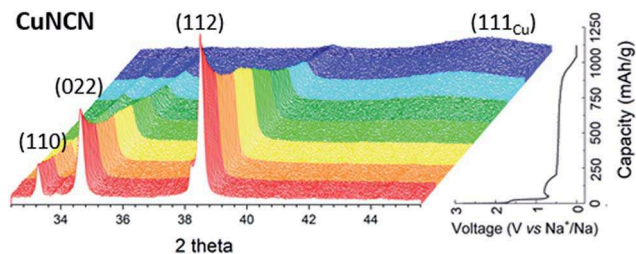


Fig. 4 The evolution of the peaks of *in situ* powder XRD data according to the first discharge of CuNCN down to $0.005 \text{ V vs. Na}^+/\text{Na}$.

to distinguish the products formed. Ongoing spectroscopic studies aim at elucidating the additional products, likely Na_2NCN , formed during the reaction.

In the first charge of CuNCN only one electron seems to be involved during the electrochemical process. The reversible capacity obtained upon cycling is closer to the theoretical capacity for the formation of Cu_2NCN (258 mA h g^{-1}) than that of CuNCN (517 mA h g^{-1}) although the formation of Cu_2NCN at the end of the charge has not been confirmed yet by any *ex situ* or *in situ* analysis. This would be in agreement with the study of the mechanism of CuO vs. $\text{Na}^+/\text{Na}^{27}$ where it was observed that during the first discharge, Cu_2O is appearing as the intermediate and suggested that the obtained reversible capacity could be due to the formation of Cu_2O upon charge. The number of electrons involved and thus the phases that are formed depends on the nature of the transition metal as well as the alkali ion being intercalated, and therefore a deeper study of each individual system is desired.

Conclusions

In conclusion, transition-metal carbodiimides MNCN ($\text{M} = \text{Cu}$, Zn , Mn , Fe , Co , and Ni) are shown for the first time to be electrochemically active in Li and Na ion batteries. Judging from the large capacity values exceeding the insertion of one alkali atom per formula unit, the hysteresis and fading of the voltage profile and given the similarities of carbodiimides to the oxide group, it seems that most M(II) binary transition-metal carbodiimides operate through conversion reactions as demonstrated by *in situ* powder XRD for CuNCN vs. Na^+/Na . Also, in comparison to the oxides, carbodiimides show higher capacities and smaller hysteresis, especially for FeNCN , CoNCN and NiNCN . This means that carbodiimides improve the electrochemical performance in terms of energy density and efficiency vs. oxides, and this opens a new field of inorganic materials that could be explored for their electrochemical performance not only in rechargeable Li and Na ion batteries but also in other electrochemical devices,²⁹ with many open questions regarding their mechanisms of reactions and future possibilities of transition-metal carbodiimides.

Notes and references

- 1 B. Dunn, H. Kamath and J. M. Tarascon, *Science*, 2011, **334**, 928.
- 2 R. Yazami and P. Touzain, *J. Power Sources*, 1983, **9**, 365.
- 3 V. Palomares, P. Serras, I. Villaluenga, K. B. Hueso, J. Carretero-González and T. Rojo, *Energy Environ. Sci.*, 2012, **5**, 5884.
- 4 V. Palomares, M. Casas-Cabanas, E. Castillo-Martínez, M. H. Man and T. Rojo, *Energy Environ. Sci.*, 2013, **6**, 2312.
- 5 B. Jache and P. Adelhelm, *Angew. Chem., Int. Ed.*, 2014, **53**, 10169.
- 6 S. Komaba, W. Murata, T. Ishikawa, N. Yabuuchi, T. Ozeki, T. Nakayama, A. Ogata, K. Gotoh and K. Fujiwara, *Adv. Funct. Mater.*, 2011, **21**, 3859.
- 7 Y. Park, D. S. Shin, S. H. Woo, N. S. Choi, K. H. Shin, S. M. Oh, K. T. Lee and S. Y. Hong, *Adv. Mater.*, 2012, **24**, 3562.
- 8 E. Castillo-Martínez, J. Carretero-González and M. Armand, *Angew. Chem., Int. Ed.*, 2014, **126**, 5445.
- 9 Y. Kim, Y. Park, A. Choi, N. S. Choi, J. Kim, J. Lee, J. H. Ryu, S. M. Oh and K. T. Lee, *Adv. Mater.*, 2013, **25**, 3045.
- 10 S. Komaba, Y. Matsuura, T. Ishikawa, N. Yabuuchi, W. Murata and S. Kuze, *Electrochem. Commun.*, 2012, **21**, 65.
- 11 A. Darwiche, C. Marino, M. T. Sougrati, B. Fraisse, L. Stievano and L. Monconduit, *J. Am. Chem. Soc.*, 2012, **134**, 20805.
- 12 H. D. Schädler, L. Jäger and I. Senf, *Z. Anorg. Allg. Chem.*, 1993, **619**, 1151.
- 13 T. D. Boyko, R. J. Green, R. Dronskowski and A. Moewes, *J. Phys. Chem. C*, 2013, **117**, 12754.
- 14 R. G. Pearson, *Chemical Hardness*, Wiley-VCH, Weinheim, Germany, 1997.
- 15 K. Morita, G. Mera, K. Yoshida, Y. Ikuhara, A. Klein, H. J. Kleebe and R. Riedel, *Solid State Sci.*, 2013, **23**, 50.
- 16 J. Cabana, L. Monconduit, D. Larcher and M. R. Palacín, *Adv. Mater.*, 2010, **22**, E170.
- 17 P. Poizot, S. Laruelle, S. Grugeon and J. M. Tarascon, *J. Electrochem. Soc.*, 2002, **149**, A1212.
- 18 P. Poizot, S. Laruelle, S. Grugeon, L. Dupont and J. M. Tarascon, *Nature*, 2000, **407**, 496.
- 19 J. M. Tarascon, S. Grugeon, S. Laruelle, D. Larcher and P. Poizot, *Lithium Batteries: Science and Technology*, ed. G. A. Nazri and G. Pistoia, Kluwer Academic Publishers, Dordrecht, 2004, p. 220.
- 20 K. Sung-Wook, D. H. Seo, X. Ma, G. Ceder and K. Kang, *Adv. Energy Mater.*, 2012, **2**, 710.
- 21 X. Liu, M. A. Wankew, H. Lueken and R. Dronskowski, *Z. Naturforsch.*, 2005, **60b**, 593.
- 22 X. Liu, L. Stork, M. Speldrich, H. Lueken and R. Dronskowski, *Chem.-Eur. J.*, 2009, **15**, 1558.
- 23 M. Krott, X. Liu, B. P. T. Fokwa, M. Speldrich, H. Lueken and R. Dronskowski, *Inorg. Chem.*, 2007, **46**, 2204.
- 24 O. Reckeweg and A. Simon, *Z. Naturforsch.*, 2003, **58b**, 1097.
- 25 X. Liu, M. Krott, P. Müller, C. Hu, H. Lueken and R. Dronskowski, *Inorg. Chem.*, 2005, **44**, 3001.
- 26 B. Milke, C. Wall, S. Metzke, G. Clavel, M. Fichtner and C. Giordano, *J. Nanopart. Res.*, 2014, **16**, 2795.
- 27 F. Klein, B. Jache, A. Bhide and P. Adelhelm, *Phys. Chem. Chem. Phys.*, 2013, **15**, 15876.
- 28 J. B. Goodenough and Y. Kim, *Chem. Mater.*, 2010, **22**, 587.
- 29 M. T. Sougrati, A. Darwiche, L. Monconduit, L. Stievano, R. P. Hermann, A. Mahmoud, M. Herlitschke, R. Dronskowski, X. Liu, *Metal Carbodiimides and Metal Cyanamides as Electrode Materials*, EP15305888, 2015.